CANMET

REPORT 80-20E

Canada Centre for Mineral and Energy Technology

Centre canadien de la technologie des minéraux et de l'énergie

AN IRIS DIAPHRAGM-BASED INTERFACE FOR USE IN ERIOMETRY

B. KIRK

MINERALS RESEARCH PROGRAM
MINING RESEARCH LABORATORIES

Canada
Energy, Mines and Resources Canada
Énergie, Mines et Ressources Canada

FEBRUARY 1980

Available in Canada through

Authorized Bookstore Agents
and other bookstores

or by mail from

Canadian Government Publishing Centre
Supply and Services Canada
Hull, Quebec, Canada K1A 0S9

CANMET
Energy, Mines and Resources Canada,
555 Booth St.,
Ottawa, Canada K1A 0G1

or through your bookseller

Catalogue No. M38–13/80-20E Canada: $2.50
ISBN 0-660-10914-X Other countries: $3.00

Price subject to change without notice.

En vente au Canada par l'entremise de nos

agents libraires agréés
et autres librairies

ou par la poste au:

Centre d'édition du gouvernement du Canada
Approvisionnements et Services Canada
Hull, Québec, Canada K1A 0S9

CANMET
Énergie, Mines et Resources Canada,
555, rue Booth
Ottawa, Canada K1A 0G1

ou chez votre libraire.

N° de catalogue M38–13/80-20E Canada: $2.50
ISBN 0-660-10914-X Hors Canada: $3.00

Prix sujet à changement sans avis préalable.

AN IRIS DIAPHRAGM-BASED INTERFACE FOR USE IN ERIOMETRY

by

B. Kirk*

ABSTRACT

Eriometry, the estimation of the size distribution of a set of fineparticles from their group diffraction pattern, has shown considerable potential for industrial application. This report describes a new and inexpensive method for interfacing the eriometer to a mini-processor. The interface consists of an iris diaphragm placed in the diffraction plane with subsequent focusing onto a single photodetector. The system has the advantage of integrating over any angular variations in the diffraction pattern without requiring a complex photodetector. The interface is applicable to the sizing of monodisperse powders as well as to the determination of size distribution of polydisperse samples. Some potential problems which may arise in the application of this technique are also investigated.

---

*Mine scientist, Elliot Lake Laboratory, Mining Research Laboratories, CANMET, Energy, Mines and Resources Canada, Elliot Lake, Ontario.

UNE SURFACE DE SEPARATION A BASE DE DIAPHRAGME IRIS POUR USAGE EN ERIOMETRIE

par

B. Kirk*

RESUME

L'ériométrie, une estimation de la granulométrie d'un jeu de particules fines de leurs franges d'interférence a fait preuve d'un potentiel considérable en ce qui concerne son application industrielle. Le présent rapport décrit une nouvelle méthode peu coûteuse pour interfacer l'ériomètre à un mini-ordinateur. L'interface est composée d'un diaphragme iris placé dans le plan de diffraction avec une mise au point ultérieur sur un seul photodétecteur. Le système a l'avantage d'intégrer sur une gamme de variations angulaires dans les franges d'interférence sans nécessiter un photodétecteur complexe. L'interface est applicable au classement volumétrique des poudres monodisperses aussi bien qu'à la détermination de la granulométrie des échantillons polydisperses. On étudie aussi certains des problèmes qui pourraient être causés par l'application de cette technique.

---

*Scientifique minier, Laboratorie d'Elliot Lake, Laboratories de recherche minière, CANMET, Energie, Mines et Ressources Canada, Elliot Lake, Ontario.

CONTENTS

TABLES

FIGURES

CONTENTS (cont'd)

ERIOMETRY AS A SIZING TECHNIQUE

The term eriometry refers to the study of diffraction patterns to obtain information on the size of small objects. The first such studies were made by Young, who used eriometric methods to compare the sizes of wool fibres and blood cells (1,2). Since then eriometry has been applied to many types of small particles known generally as fineparticle systems. The term "fineparticle" was introduced by B.H. Kaye to distinguish between microscopic fragments of bulk materials and the usual meaning of "particles" in physics, such as the electron, proton, neutron, etc. This serves as an aid in differentiating the two cases, particularly in computer search systems, and is used throughout this report.

Eriometry consists of setting up an optical system in such a way as to form the Fraunhofer diffraction pattern of the fineparticles under study. In principle, by making appropriate measurements of the diffraction pattern with reference to a previously determined calibration, the size distribution of the fineparticles can be determined. Problems have arisen in the past, however, with the complexity of the data so obtained. When a monodisperse system of fineparticles of reasonably regular shape is under study, the diffraction pattern is usually fairly simple and the data analysis straightforward. However, if the system of fineparticles is polydisperse, the diffraction pattern quickly increases in complexity and the data analysis becomes correspondingly more difficult. For this reason, eriometry has been limited in the past to the study of monodisperse systems, usually under controlled laboratory conditions. With the advent of the minicomputer, and, more recently, of the microprocessor, the technique is becoming practical for application to polydisperse systems in the industrial environment.

Eriometry is attracting widespread interest and is finding applications in almost all facets of industry, resulting in the development of several commercial instruments (3,4,5,6,7). Notable among these are the Leeds & Northrup Microtrac and the Cilas Granulometer (8,9,10). Most of the interest in such instruments stems from a need for the rapid acquisition of information on fineparticle size distribution with possible feedback for process control. For example, two such applications, although distinctly different, arise in the mining industry.

In the grinding of ore by ball, rod, or similar type of mill, there is a need for precise control of grain size. The processes whereby the minerals are extracted from the ore depend very sensitively on having materials within a well defined size range. Ore breakage consumes a substantial fraction of the total energy requirements and it has been estimated that better grinding control could reduce energy costs by as much as 15% (3).

The conventional method of analyzing slurry is to extract a small sample from the mill which is examined microscopically or by sedimentation techniques to determine the particulate size distribution. Such methods are generally slow and depend on the sample being truly representative. If grinding is stopped while the sample is being analyzed valuable grinding time is lost. On the other hand, if the mill continues operating while the sample is analyzed, the analysis results may not represent true conditions.

An alternative approach would be to design an eriometric system to yield continuous, real-time information on the grinding process with samples being taken while the mill is operating. Because the operation is not stopped better mixing would be assured with a consequently higher probability of obtaining a representative sample. The specimen would be pumped into a chamber fitted with windows for illumination by a laser. The diffraction pattern formed by the fineparticles could be interfaced to a miniprocessor for immediate analysis. The sample would then be returned to the mill for further grinding if required. Feedback from the eriometer would possibly control various factors in the milling process, such as dilution, grinding rate and time. Such a system must be designed to take into account problems such as air bubble formation and deposition on the windows; these,

however, are essentially fluid flow problems which, although complex, may be dealt with through proper system design.

Another potential application of eriometry in the mining industry is for measuring the quantity and size distribution of airborne dust. The current methods of monitoring airborne dust generally fall into one of two categories: dust particle number and dust mass techniques (11). None of these methods yield real-time, continuous information. Some yield average values by integrating the information over an extended time period. The analysis of the samples collected with these methods is usually complicated and time consuming. Those techniques which yield results quickly usually give only instantaneous values.

An eriometer could be used to obtain real-time size distribution information on airborne dust. In fact, one such instrument, developed by Talbot amounted to one of the first attempts at analyzing complex diffraction patterns (2,12). In Talbot's eriometer, gold mine dust samples were collected on a glass slide by precipitation. The slide was then shadow coated with aluminum metal by vacuum evaporation and deposition. The dust was washed off, leaving a fineparticle replica in an otherwise opaque aluminum film. By illuminating this replica with the light from a mercury vapour lamp, the Fraunhofer diffraction pattern was formed on a prepared photographic transparency. This transparency was used to sample the diffraction pattern and to acquire size distribution information.

Talbot's eriometer did not gain widespread acceptance, primarily because of the technological difficulties involved in depositing a thin metal film of suitable thickness. Furthermore, to use the prepared transparency as an interface, some assumptions had to be made a priori about the expected distribution and range of fineparticle sizes. This is not always practical as the size distribution of airborne dust can often change radically over a very short time period.

This instrument did not, in fact, give a real-time analysis of airborne dust. It amounted, essentially, to a novel method for analyzing dust particles collected by existing techniques.

With the advent of the laser and the miniprocessor, an eriometer may now be designed to assess dust levels in a continuous, reliable manner. Rather than collect the fineparticles on a slide for subsequent analysis, the size distribution may be determined by analyzing them while they are in transit through the eriometer.

These two applications of eriometry both require an interface between the optical system and the data manipulation system. However, the type of interface required is different in the two cases.

The milling process represents essentially a quality control problem. As such it is not necessary to know the size distribution exactly. It is more important to know if the size distribution falls within predefined limits and if it is changing. This, then, may be regarded as a static analysis problem and requires some form of fixed interfacing.

It is conceivable that an analysis of airborne dust for assessment of its health hazard could be done with the same interfacing technique. In this case it is required to determine how many fineparticles within a given size range are present e.g., the so-called respirable fraction. In general, however, it may be desirable to determine the size distribution as accurately as possible. This is more difficult as the size distribution is probably far from being static. The number of fineparticles in any size range can change very rapidly and this will alter the structure of the diffraction pattern significantly. It would be possible to deduce from preliminary investigations the approximate size range of dust particles present under given circumstances. However, it would be impractical to do this for every situation normally encountered in industry. It is not, therefore, feasible to have a complete set of interchangeable fixed interfaces for airborne dust measurement and some form of dynamic interfacing is required.

It is this problem with interfacing to a data processor which currently limits the effectiveness of eriometry as a dust analysis tech-

nique. Accordingly, the present work concentrated on the development of an effective, low-cost, dynamic interface. The theoretical structure of the diffraction pattern data matrix as well as the design and use of the interface are discussed.

THE DATA MATRIX

When a parallel beam of monochromatic coherent light is incident on a fineparticle, the light is scattered in a well defined manner. If the fineparticle diameter is somewhat larger than the wavelength of the light, then in the far-field zone, the scattered light forms the Fraunhofer diffraction pattern of the fineparticle. The Fraunhofer conditions can be stated as:

$$\frac{D^2}{2Z} << \lambda \text{ and } D > \lambda$$

where the variables are defined as in Eq 1. The far-field condition can normally be met by forming the diffraction pattern at the focal plane of a converging lens known as the Fourier Transform lens. The Fraunhofer diffraction pattern formed by an object is the Fourier Transform of the object. Hence, the converging lens which forms the Fraunhofer diffraction pattern is called a Fourier Transform lens. This lens will focus any light diffracted at a given angle to the same point in the diffraction plane, regardless of the scattering object's position. Thus, if a fineparticle moves across the path of the incident beam, the diffraction pattern will not change.

If the object under study is a sphere, the Fraunhofer diffraction pattern formed will be the well known Airy disc pattern. The intensity distribution is described by the equation found in any standard optics text (13,14):

$$I(\rho) = I_o \left[\frac{2J_1(\pi D\rho/\lambda Z)}{(\pi D\rho/\lambda Z)}\right]^2 \qquad \text{Eq 1}$$

where $I(\rho)$ = intensity at radius ρ

I_o = intensity at $\rho = 0$

D = particle diameter

ρ = radius in diffraction plane

λ = wavelength of illuminating radiation

Z = focal length of Fourier Transform lens

J_1 = Bessel function of the first kind and of order 1

This function is depicted in Fig. 1.

If, instead of a single fineparticle, there are N fineparticles arranged at random over the extent of the incident beam, then the diffracted intensity is N times the intensity from one fineparticle (14). It has been shown by Talbot that this holds true provided the number of fineparticle pairs separated by less than a few wavelengths is small (15).

The foregoing has been in terms of spherical particles. If the fineparticles are not spheres, the resulting diffraction pattern will still display circular symmetry provided there is a large number of randomly oriented fineparticles. Effectively, this means that all angles in the plane of the sample must be equally

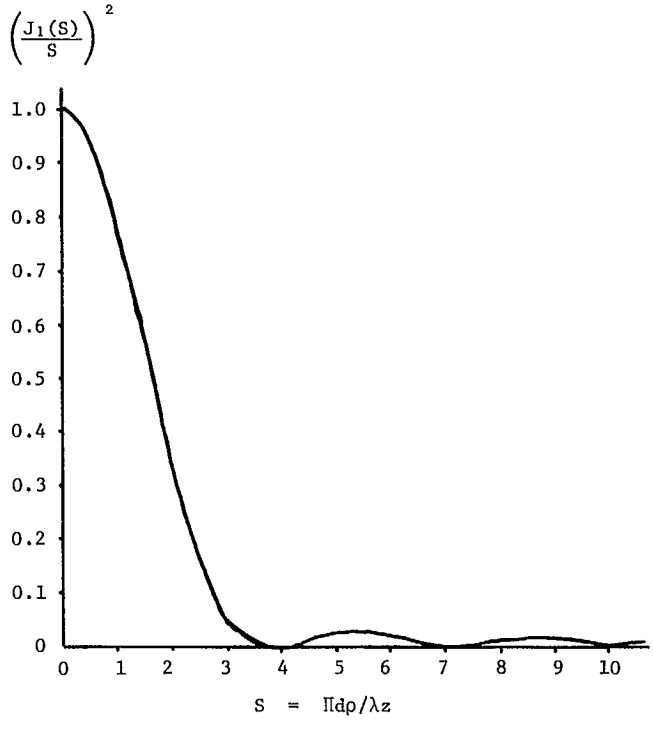

Fig. 1 - Airy pattern

represented. There are, of course, practical limitations to this, as the number of fineparticles must remain finite, and extremely irregular shapes may have a preferred orientation while moving in a fluid stream. This often results in the diffraction pattern having a grainy appearance.

Measurement of the intensity distribution in the diffraction pattern could be used to determine size of the fineparticles. This size would actually be the diameter of a sphere which would give the same intensity distribution. Particularly for extremely irregular shapes, e.g., fibres, care would be needed in interpreting results.

In practice it is very difficult to make accurate measurements of light intensity, although this has been done in some systems (16,17). An intensity measurement requires that the detector be as small as possible, which may result in a poor signal to noise ratio. A more practical approach is to measure the total energy falling within a specified area of the diffraction pattern.

Equation 1 can be integrated to yield the energy falling within any radius ρ:

$$L(\rho) = E\,[\,1 - J_o^2(\Pi D\rho/\lambda Z) - J_1^2(\Pi D\rho/\lambda Z)\,] \qquad \text{Eq 2}$$

where J_o = Bessel function of the first kind and of order 0

which is shown in Fig. 2.

It is this energy function which is ultimately to be interfaced to the data processor in some manner.

For any annular area bounded by radii ρ_1 and ρ_2, where $\rho_2 > \rho_1$, the total diffracted energy from a monodisperse collection of fineparticles is:

$$\Delta L(\rho_1,\rho_2) = E\,[J_o^2(\Pi D\rho_1/\lambda Z) + J_1^2(\Pi D\rho_1/\lambda Z) - J_0^2(\Pi D\rho_2/\lambda Z) - J_1^2(\Pi D\rho_2/\lambda Z)\,] \qquad \text{Eq 3}$$

The E appearing in Eq 2 and 3 is the energy incident upon the fineparticles and is given by:

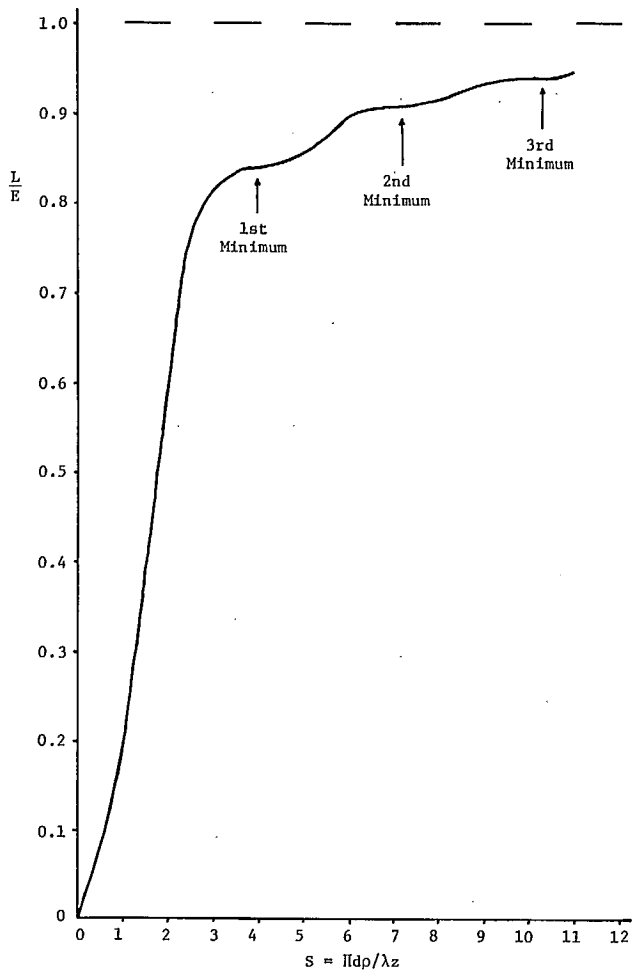

Fig. 2 - Total energy distribution in Airy pattern

$$E = E_o N \Pi \frac{D^2}{4} \qquad \text{Eq 4}$$

where E_o is the energy per unit area or intensity, of the incident beam.

Equation 4 expresses the energy in terms of the number of fineparticles. It could equally well be expressed in terms of any other parameter dependent on the diameter; such as surface area or volume and hence mass. For present purposes, the use of fineparticle number will be assumed.

If the collection of fineparticles is polydisperse, the light energy in any ring is the sum of the contributions from all sizes:

$$\Delta L(\rho_1,\rho_2) = \frac{E_o \Pi}{4} \sum_{i=1}^{M} N_i D_i^2\,[J_o^2(\Pi D_i\rho_1/\lambda Z) + J_1^2(\Pi D_i\rho_1/\lambda Z) - J_o^2(\Pi D_i\rho_2/\lambda Z) - J_1^2(\Pi D_i\rho_2/\lambda Z)] \qquad \text{Eq 5}$$

where N_i is the number of fineparticles of diameter D_i and M is the number of sizes.

This equation may be expressed in matrix notation as:

$$L_i = N_j T_{ij} \qquad \text{Eq 6}$$

where L_i is the energy distribution and T_{ij} is a matrix of coefficients linking the energy distribution to the fineparticle size distribution via the interface (18). Note that in Eq 6, the term $E_o \pi D_i^2/4$ has been absorbed into the T_{ij} matrix.

This matrix equation can be rewritten as:

$$N_j = L_i T_{ij}^{-1} \qquad \text{Eq 7}$$

The inversion matrix, T_{ij}^{-1}, can be determined by calculation or by calibration with known quantities of monosized spheres and can be stored in a miniprocessor. Measurements of L_i can then be used in computation to determine N_j.

Felton has used the approach of assuming a particular distribution function and adjusting the parameters to obtain a best fit (19). This is useful for saving computation time and avoids problems with negative values of N_j. Kaye has pointed out that this method may result in gross errors if the distribution is monodisperse or bimodal (1).

An alternative approach is to scan the values of L_i to find the maximum value of ρ which has an energy significantly different from the background. Assuming that this ring arises only from those fineparticles which contribute the most energy to this annulus of the diffraction pattern, the size range of these fineparticles can be calculated. Implicit in this is the notion of using only the central maximum of the diffraction pattern to obtain size distribution information. This first order transformation is based on the fact that approximately 84% of the energy is in the central lobe with only small amounts in the subsidiary rings. The entire energy distribution within this central maximum can be computed, normalized to the observed annulus, and subtracted from the observed energy distribution. Using this normalized calculated distribution, the relative number of particles in this size range can be computed from Eq 4, i.e., $N \alpha E/D^2$ where D is the average fineparticle size in the range. Computation then moves to the next smallest annulus and the procedure is repeated for each size range. The size data can be normalized to give a discrete distribution histogram or a cumulative distribution curve. The complete analysis procedure is given in the Appendix.

This approach assumes there is no significant overlapping of diffraction orders. The effects of this assumption will be discussed later.

The foregoing is based on the idea of sampling annular areas of the diffraction pattern. This is most easily done at the interface.

There have been a few instruments developed using an interface which samples only a small angular segment of the diffraction pattern. Although this is useful for obtaining information proportional to various powers of the diameter, these instruments suffer from the disadvantage that they do not measure a complete annulus of the diffracted light (9). As mentioned earlier, the patterns are usually somewhat grainy and the resulting low signal to noise ratio will have an effect on accuracy of the results. It is more advantageous to measure the energy falling within a complete annulus as a single measurement. This results in an integration over any variations in signal strength with angle.

Previously developed methods have divided the area of the diffraction pattern into annular segments by physical construction of the interface. An annular iris diaphragm, a photodiode array and a fibre-optic array have all been used to sample an entire annulus (20,21). All of these methods are relatively expensive and difficult to construct.

Another approach is to leave the division of the diffraction pattern into annular rings as a task for the data processing equipment. In such a system, an ordinary optical iris diaphragm is placed in the diffraction plane. The diffraction pattern is then focused down to a single photodetector. The diaphragm is gradually

closed and the total light energy is recorded as a function of radius. In effect, this results in a series of measurements, each having $\rho_1 = 0$ and a different value of ρ_2 in Eq 5. The differentiation is then carried out as part of the data processing.

This approach has the advantage of very low cost. Furthermore, being a continuously variable radius interface, the size of the steps over which discrete measurements are made can be varied as required to suit the needs of a particular task. Because the entire diffraction pattern is sampled, the signal to noise ratio should be reasonably high.

The design of an optical system using an iris diaphragm as an interface to a measurement system has been investigated. This design, along with some experimental results are discussed below.

THE DESIGN AND USE OF THE INTERFACE SYSTEM

DESIGN OF THE OPTICAL SYSTEM

The optical system employed in this work is shown in Fig. 3 and 4. The apparent curvature in the system as seen in Fig. 4 is an artifact of the photography. Light from a helium-neon laser (λHe-Ne = 0.6328 μm) was passed through a beam expander and spatial filter. In addition to removing unwanted noise from the beam, this ensured that a large number of fineparticles would be in the path of the beam. Except for purposes of calibration, the fineparticles studied were irregular in shape and it was necessary to have many random orientations.

The samples were prepared by placing a small quantity of powder in a specially constructed cell intended primarily for microscope counting of dust samples collected by impinger (11). The cell consisted of a 2 mm thick microscope slide with a well in the centre having dimensions 50 mm long, 20 mm wide and 1.0 mm deep. The well was then filled with water and a second microscope slide was used to cover it. The cell was sealed shut with melted wax. The sample was placed in a holder in the eriometer for analysis.

After being diffracted by the fineparticles, the light was focused by the Fourier Transform lens onto the iris diaphragm, the first stage of the interface. A small beam stop was

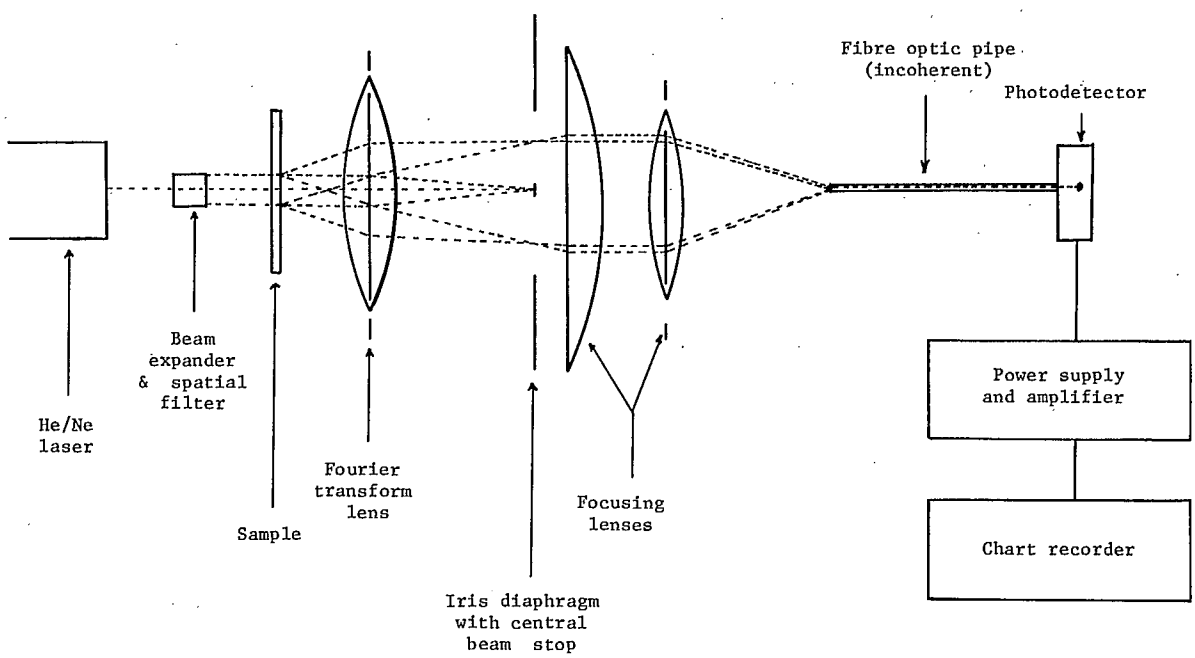

Fig. 3 - The eriometer system (schematic)

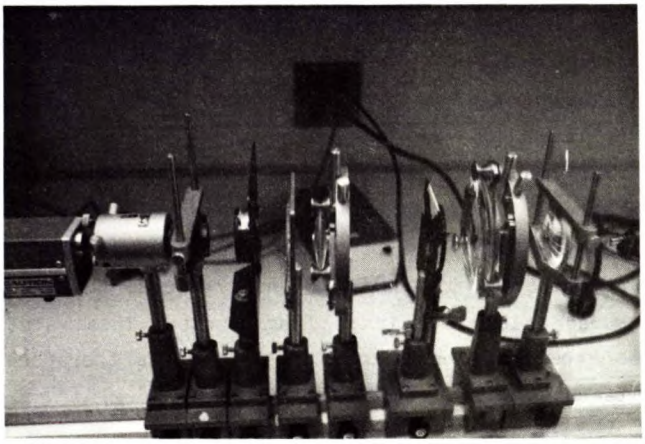

Fig. 4 - The eriometer system (photograph)

placed in the plane of the diaphragm to remove the central beam of undiffracted light. The subsequent lens system was used to focus the remaining light onto one end of a fibre-optic bundle 2.5 mm in diameter. The other end of this bundle was coupled to a single photosensitive detector and chart recorder.

When the system was in use, the diaphragm was closed in discrete steps and the energy recorded for each. The range of available sizes was from ρ = 1 mm to ρ = 23 mm.

The eriometer was first calibrated using monodisperse latex spheres. It was then applied to determining the size of monodisperse, approximately spherical fineparticles-Lycopodium spores. Measurements were then made on polydisperse, irregular fineparticles - silica and diamond dusts. Each of these will be discussed separately.

It was observed early in this work that this interfacing technique was capable of distinguishing between monodisperse and polydisperse samples. Monodisperse samples result in the diffraction pattern having a very definite ring structure with visible maxima and minima, provided the fineparticles are not extremely irregular in shape and can be classified as "rough spheres". Polydisperse samples yield diffraction patterns which do not display this structure. They are more continuous from a central maximum to a non-zero minimum at some radius. These two types of patterns can be recognized and treated differently in the analytical process. It is therefore possible to determine the size of a monodisperse sample with a high degree of accuracy as well as the size distribution of a polydisperse sample.

CALIBRATION

In using the eriometer to determine size distributions, it is essential that the optical path length, Z, be known as accurately as possible. This was determined by using monodisperse latex spheres which had been microscopically sized at 9.69 µm. These spheres resulted in the diffraction pattern showing very distinct maxima and minima as seen in Fig. 5. The central section of this photograph was overexposed in order to show the fainter outer rings. The band of light running vertically through the diffraction pattern is a result of photographic defects.

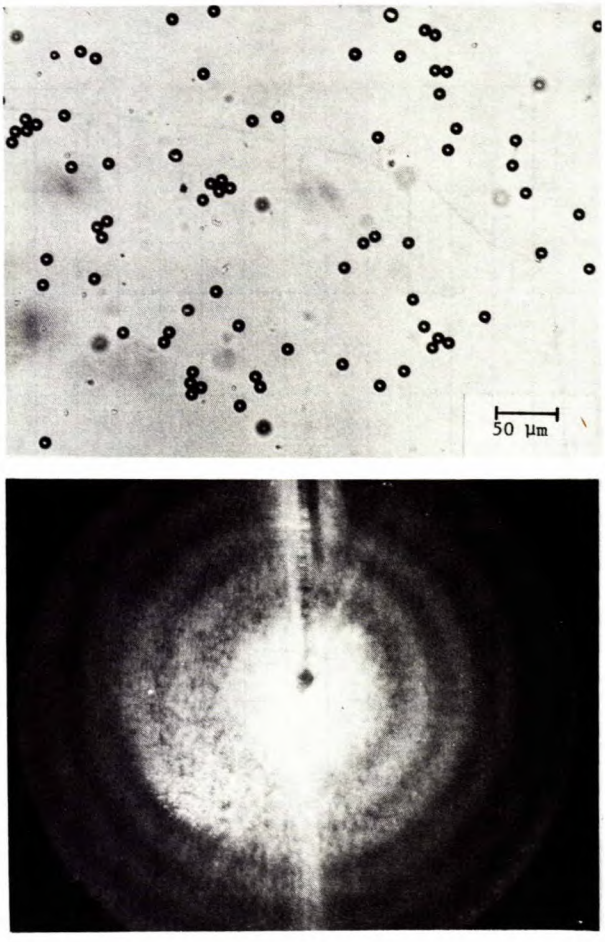

Fig. 5 - 9.69 µm latex spheres and diffraction pattern

To determine the path length, the diaphragm was closed to each succeeding visible minimum in the diffraction pattern. To determine the positions of the minima as accurately as possible, the transmitted energy values were recorded on the chart recorder. The position of each minimum was taken as the point of minimum slope as visually determined from the graph (Fig. 6).

From these values of the aperture radius, the path length was determined as follows. The Bessel function $J_1(S)$ has a zero value only when its argument:

$$S = \frac{\pi D \rho}{\lambda Z} \qquad \text{Eq 8}$$

has definite values. Therefore, for each minimum, the value of Z can be calculated from:

$$Z = \frac{\pi D \rho}{\lambda S} \qquad \text{Eq 9}$$

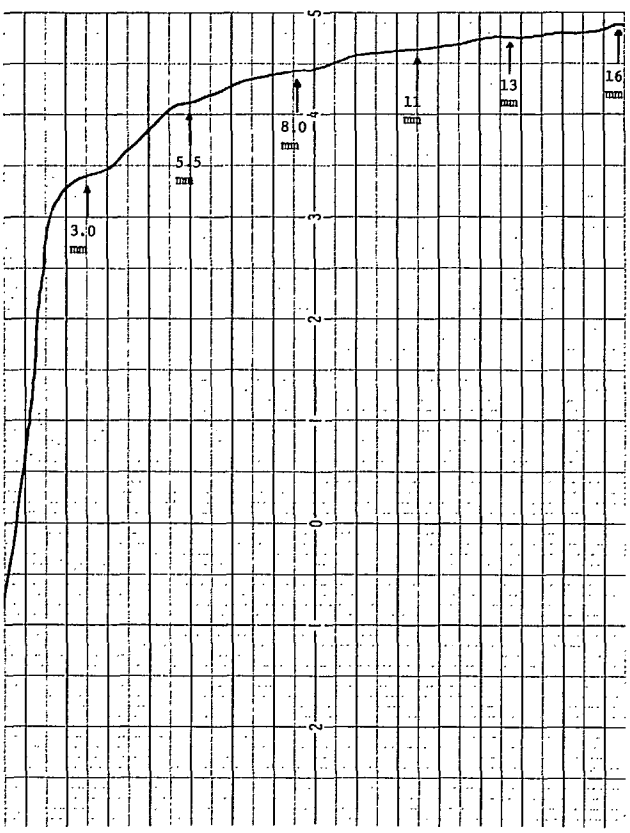

Fig. 6 - Experimentally measured energy distribution in diffraction pattern of 9.69 μm latex spheres

The results of this calibration are given in Table 1 for the first three minima. The value of 37.7 mm for Z was used to predict the positions of the subsequent three minima. The predicted and measured positions are given in Table 2. Considering the subjective nature of choosing the point of minimum slope, particularly at these low intensities, the predicted and measured values are in good agreement. This value of the path length of Z = 37.7 mm was therefore taken as a calibrated value.

Table 1 - Calibration of optical path length, Z (D = 9.69 μm; λ = 0.6328 μm)

Minimum No.	S	ρ (mm)	Z (mm)
1	3.832	3.0	37.66
2	7.016	5.5	37.71
3	10.173	8.0	37.83
			Z = 37.7 mm

Table 2 - Comparison of predicted and measured positions of minima (D = 9.69 μm; λ = 0.6328 μm; Z = 37.7 mm)

Minimum No.	S	Predicted ρ (mm)	Measured ρ (mm)	Δρ/ρ (%)
4	13.324	10.5	11	4.8
5	16.471	12.9	13	0.8
6	19.616	15.4	16	3.9

MONODISPERSE, APPROXIMATELY SPHERICAL FINEPARTICLES

In most applications, the fineparticles to be studied will not be spherical. Furthermore, the interface diaphragm would operate in discrete steps rather than continuously. As a first stage in investigating the suitability of the iris diaphragm as an interface for the study of irregular fineparticles, the eriometer was applied to the problem of determining the size of Lycopodium spores. These particles can be classified as rough spheres, as seen in Fig. 7.

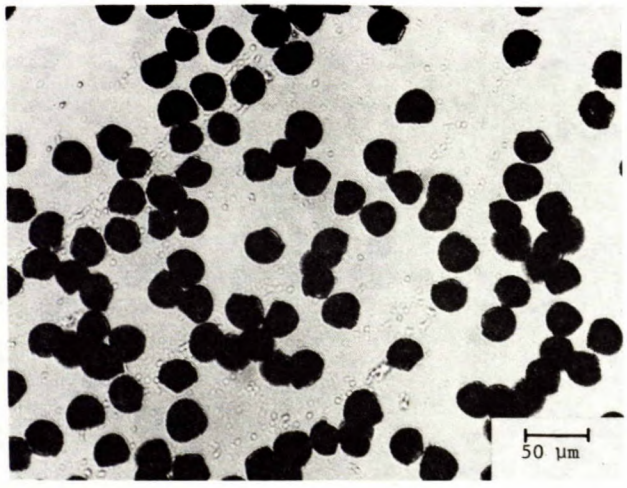

Fig. 7 - Lycopodium spores

Lycopodium spores will absorb large quantities of water and will increase in diameter. For this reason, the size of the spores was measured microscopically before the sample was dispersed in water. The eriometric analysis was carried out immediately after the dispersion of the powder. Further microscopic examination of the sample after 24 h showed an increase in spore diameter of approximately 20%.

The diaphragm was set to full aperture and the photodetector amplifier was adjusted to give a reading of 100 arbitrary units. The aperture was slowly reduced until the output reading was observed to decrease. The diaphragm was then closed in steps of 0.5 mm ($\Delta\rho$) and a reading was taken at each step. These results are given in Table 3. The values of ΔL were used to determine the positions of the minima, which in turn were used to calculate the powder diameter as shown in Table 4.

An error will arise if an incorrect order is assigned to a minimum. There are two possible causes for this. One or more minima may be contained within the innermost sampling area of the interface, particularly for large fineparticles. Furthermore, at larger radii, a single annulus may span across a minimum with no appreciable reduction in energy if it also takes in a large portion of the maximum on either side. This difficulty can be dealt with by comparing the ratio in radii for two minima with the ratio in theoretical values of S, i.e.,

$$\frac{\rho_i}{\rho_j} = \frac{S_i}{S_j} \qquad \text{Eq 10}$$

The best fit gives the orders of the minima as has been done in Table 4.

The size of the spores as determined by the eriometer is 29 ± 6 µm, microscope sizing yielded a value of 30 ± 5 µm. The large uncertainty in the eriometer results stems mostly from the actual spread in particle sizes and also from the coarse step size in the interface. The actual position of a minimum may lie anywhere within this range, thereby introducing a degree of error. However, as the particles were observ-

Table 3 - Eriometer data for Lycopodium spores
(λ = 0.6328 µm; Z = 37.7 mm)

ρ (mm)	L (arb)	ΔL (arb)
10.0	100	0.5
9.5	99.5	0
9.0	99.5	0.2
8.5	99.3	0.3
8.0	99.0	0.5
7.5	98.5	1.0
7.0	97.5	0
6.5	97.5	0.2
6.0	97.3	0.8
5.5	96.5	0.5*
5.0	96.0	1.5
4.5	94.5	1.0*
4.0	93.5	1.8
3.5	91.7	2.7
3.0	89.0	1.5*
2.5	87.5	2.0
2.0	85.5	4.0
1.5	81.5	2.0*
1.0	79.5	79.5

* indicated minima

Table 4 - Determination of diameter of Lycopodium spores

ρ (mm)	Minimum No.	S	D (µm)
1.5	2	7.016	35.6
3.0	3	10.173	25.8
4.5	5	16.471	27.8
5.5	6	19.616	27.1

D = 29 µm ± 6 µm

ed microscopically to have a range of ± 5 μm in diameter, a finer step size would probably not result in a more precise value in this case.

POLYDISPERSE IRREGULAR FINEPARTICLES

The eriometer was applied to the determination of the size distributions for two different types of irregularly shaped fineparticles. The first type consisted of four silica samples: BCR 66, 67, 69 and 70. The size distributions of these materials have been examined and certified on the basis of sedimentation measurements (22). These powders, as seen in Fig. 8-11 exhibit a high degree of surface roughness and are not spherical. Many of the fineparticles have sharp edges and concave surface features. The aspect ratio for these samples - ratio of maximum to minimum diameter for a given fineparticle - ranged from 1.1:1 to 2.0:1.

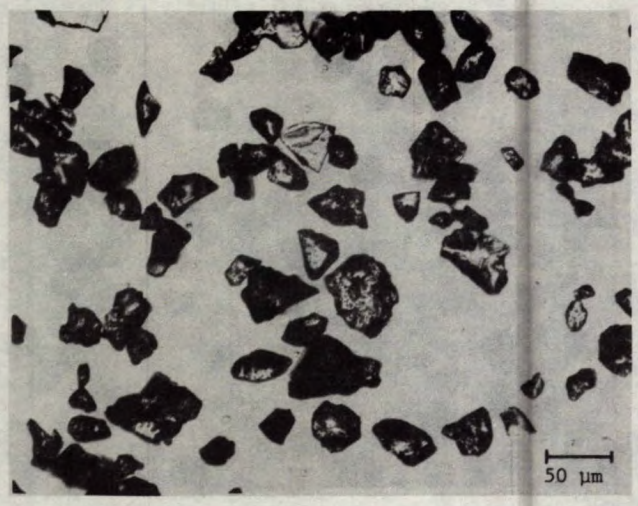

Fig. 10 - Silica sample, BCR 69

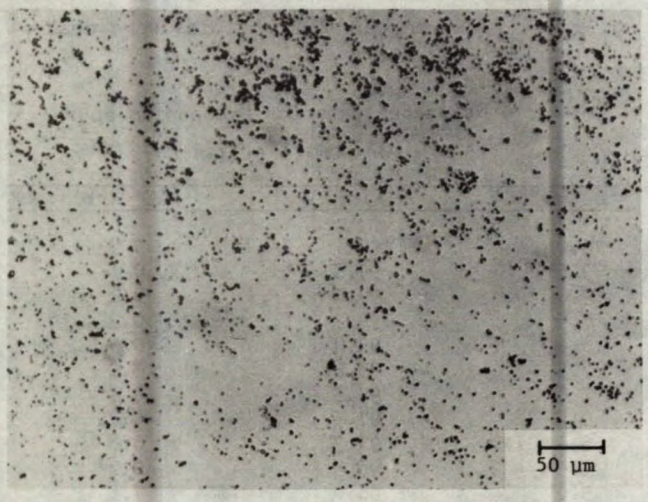

Fig. 8 - Silica sample, BCR 66

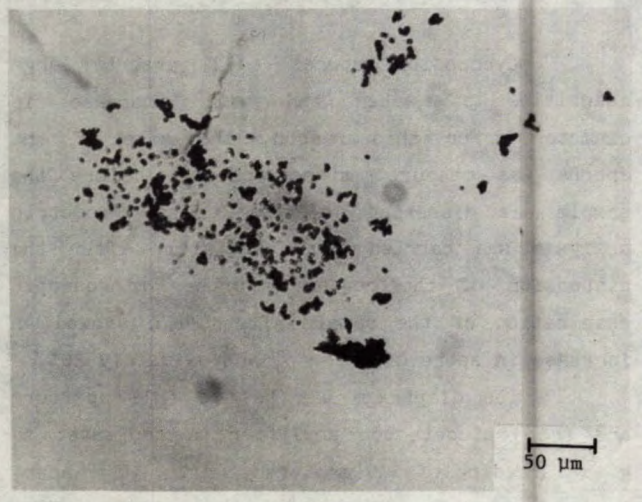

Fig. 11 - Silica sample, BCR 70

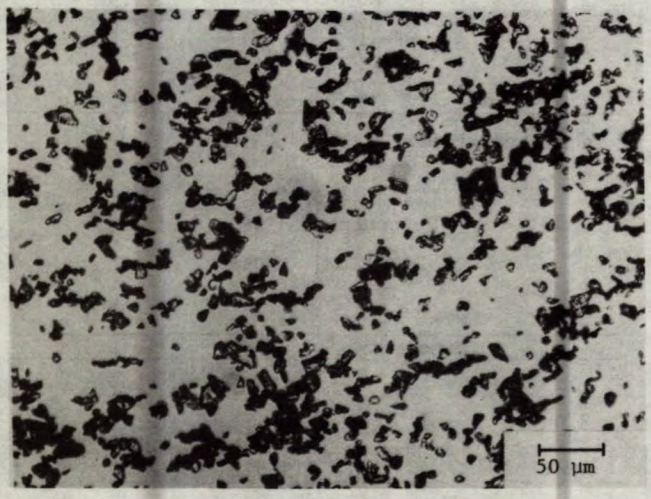

Fig. 9 - Silica sample, BCR 67

The second material to be studied consisted of presized diamond fragments in the size ranges of 4 to 12 μm, 6 to 12 μm, and 20 to 40 μm. These fineparticles were extremely irregular as seen in Fig. 12 through 14, with aspect ratios ranging from 1.1:1 to 3.5:1.

Because these powders are polydisperse and irregular, their diffraction patterns do not exhibit a definite ring structure. The size distribution in terms of equivalent spheres could be

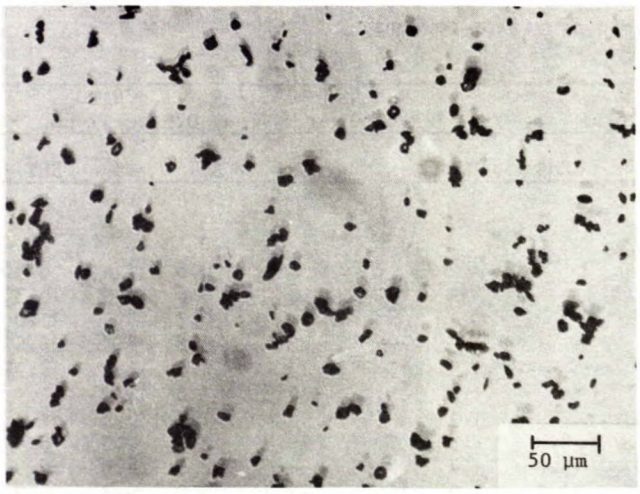

Fig. 12 - 4-12 µm diamond dust

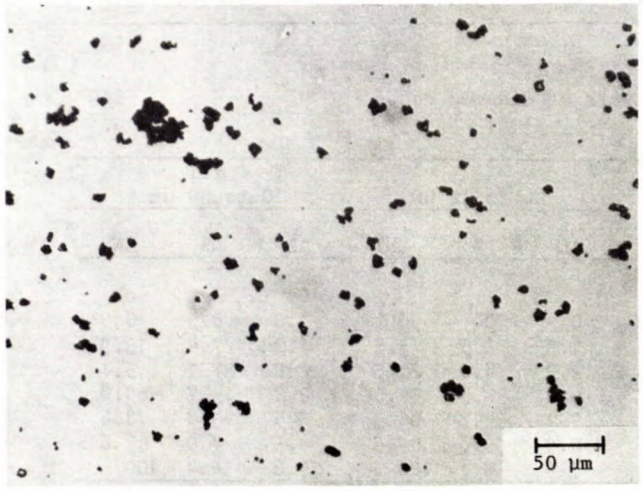

Fig. 13 - 6-12 µm diamond dust

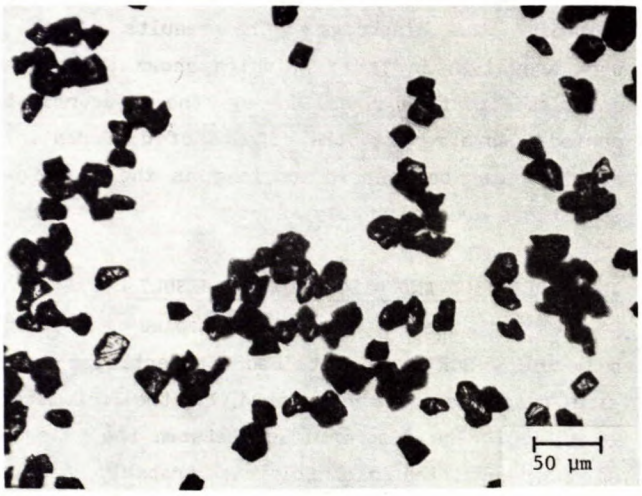

Fig. 14 - 20-40 diamond dust

determined, however, by the following analysis steps:

1. The diaphragm was closed until the transmitted energy was observed to decrease significantly. This level of significance was set at 0.5%; the lowest detectable limit on the chart recorder.
2. The diaphragm was closed in 1 mm ($\Delta\rho$) steps with the transmitted energy being recorded at each step.
3. The energy difference for each annulus was determined from the collected data.
4. The size range and number of fineparticles corresponding to each annulus was calculated as discussed earlier on the basis of a first order transformation.

The size range for each annulus was taken as that which contributes the most energy to the annulus. It has been shown by Felton (19) and Robb (23) that this size is given by:

$$D = \frac{1.357\ \lambda Z}{\Pi\rho} \qquad \text{Eq 11}$$

This size is approximately one third that of a fineparticle which has a minimum at the annulus and results from a combination of annular area effects and the shape of the Airy distribution. To calculate the number of fineparticles contributing to the innermost annulus, the upper size limit was arbitrarily set to 100 µm for computing purposes.

The results of this analysis are given in Table 5 for the silica powders and Table 6 for the diamond dusts. The calculated distribution curves are shown in Fig. 15 through 21 which also show the cumulative distribution curves from the published data for the silica samples (22). These published data give the cumulative curves in per cent undersize by mass. These have been converted to per cent undersize by number for comparison purposes, with the assumption that the particles are spheres, i.e., $N \alpha m/D^3$; m = mass. These curves are shown as the heavy broken lines in Fig. 5-8. In all the distribution curves, the fractions above 10 µm are shown only where significant.

Table 5 - Eriometric analysis of silica powders

Ring range mm		Size range µm		BCR 66 0.35 to 2.5 µm			BCR 67 3 to 20 µm			BCR 69 12 to 90 µm			BCR 70 0.5 to 12 µm		
Max	Min	Min	Max	ΔL	N%	ΣN%	ΔL	N%	ΣN%	ΔL	N%	ΣN%	ΔL	N%	ΣN%
16	15	0.64	0.67	0	0	0									
15	14	0.67	0.74	0.5	0.3	0.3							0	0	0
14	13	0.74	0.78	0.7	15.3	15.6							0.5	8.4	8.4
13	12	0.78	0.85	0.8	5.0	20.6							0.6	7.9	16.3
12	11	0.85	0.92	0.9	8.0	28.6							0.7	4.7	21.0
11	10	0.92	1.03	1.3	18.7	47.3				0	0	0	0.8	4.6	25.6
10	9	1.03	1.13	1.8	9.6	56.9				0.5	13.2	13.2	1.5	13.3	38.9
9	8	1.13	1.27	2.0	8.3	65.2	0	0	0	1.0	21.1	34.3	1.6	12.0	50.9
8	7	1.27	1.49	2.1	6.1	71.3	0.5	2.1	2.1	1.1	14.5	48.8	1.7	0.5	51.4
7	6	1.49	1.74	2.2	9.3	80.6	0.6	2.8	4.9	1.3	7.5	56.3	2.1	7.5	58.9
6	5	1.74	2.05	2.3	4.7	85.3	0.8	11.7	16.6	1.4	0.4	56.7	2.5	8.0	66.9
5	4	2.05	2.58	2.4	7.0	92.3	1.2	15.5	32.1	2.0	15.0	71.7	3.0	9.3	76.2
4	3	2.58	3.43	2.5	2.5	94.8	4.5	20.9	53.0	3.6	10.3	82.0	4.0	11.0	87.2
3	2	3.43	5.17	2.7	2.6	97.4	8.0	25.4	78.4	5.0	10.3	92.3	5.5	7.1	94.3
2	1	5.17	10.3	4.2	1.0	98.4	17.0	15.2	93.6	6.2	3.5	95.8	5.6	2.5	96.8
1	0	10.3	∞	73	1.6	100	67.4	6.4	100	73.9	4.2	100	69.4	3.2	100

Table 6 - Eriometric analysis of diamond dusts

Ring range mm		Size range µm		I 4 to 12 µm			II 6 to 12 µm			III 20 to 40 µm		
Max	Min	Min	Max	ΔL	N%	ΣN%	ΔL	N%	ΣN%	ΔL	N%	ΣN%
8	7	1.27	1.49	0	0	0				0	0	0
7	6	1.49	1.74	1.0	3.4	3.4	0	0	0	1.0	6.5	6.5
6	5	1.74	2.05	1.1	1.2	4.6	1.3	3.5	3.5	1.2	7.4	13.9
5	4	2.05	2.58	2.5	23.8	28.4	2.0	18.0	21.5	2.0	37.1	5.1
4	3	2.58	3.43	6.0	25.7	54.1	6.7	32.5	54.0	2.2	13.7	64.8
3	2	3.43	5.17	10.0	37.9	92.0	9.2	32.3	86.3	2.5	13.8	78.6
2	1	5.17	10.3	11.0	1.0	93.0	10.9	5.6	91.9	4.3	7.0	85.6
1	0	10.3	∞	68.4	7.0	100	7.9	8.1	100	79.8	14.4	100

Because of the polydisperse nature of these samples there was a possibility that the size distribution of the material within the area of the incident beam would change during the measurement period. The largest fineparticles would settle out faster than the smallest ones and this differential settling could cause a shift in the distribution curves. It must be remembered, however, that the time required for the analysis of a single sample was relatively short - about a minute to a minute and a half. It was believed that this time was short enough so that the effects of differential settling of the fineparticles would be negligible. To test this conjecture, two samples - BCR 67 and diamond dust I of 4 to 12 µm - were analyzed by closing the diaphragm as discussed earlier and then by reopening the diaphragm. The results of this work are given in Table 7, which shows there are no significant changes during the measurement period. As a result, the effects of differential settling can be ignored as long as the measurement times are reasonably short.

INTERPRETATION AND DISCUSSION OF RESULTS

Of the four silica samples analyzed, only one - BCR 67 - contained fineparticles in a size range completely covered by the eriometer (Fig. 16). The discrepancies between the measured and certified distributions probably result from the different analysis techniques used to acquire the two sets of data. Eriometry and sed-

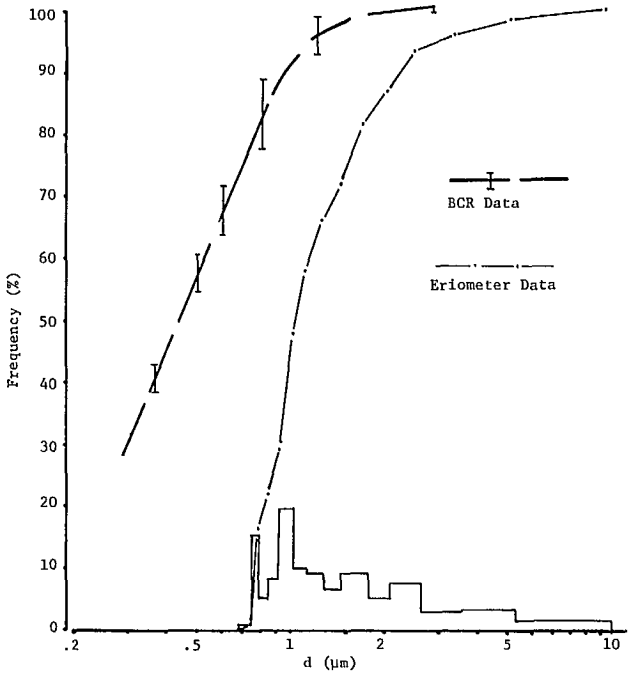

Fig. 15 - Distribution for silica sample, BCR 66

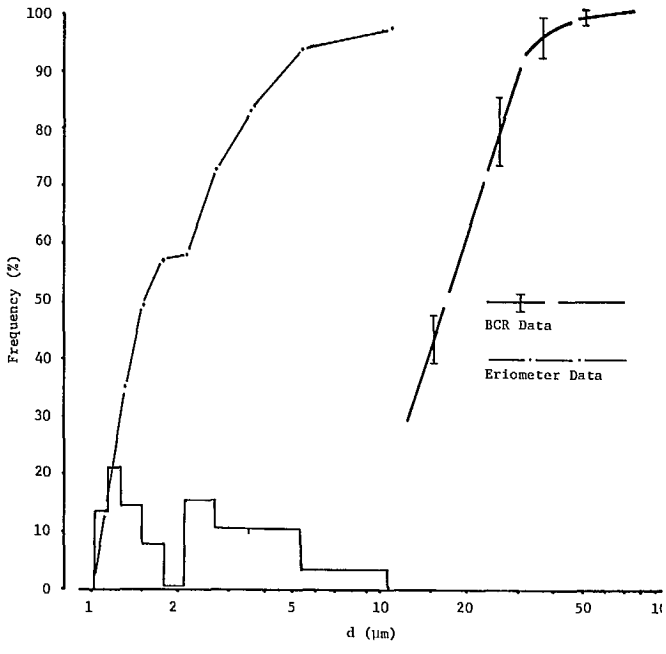

Fig. 17 - Distribution for silica sample BCR 69 (with Z = 37.7 mm)

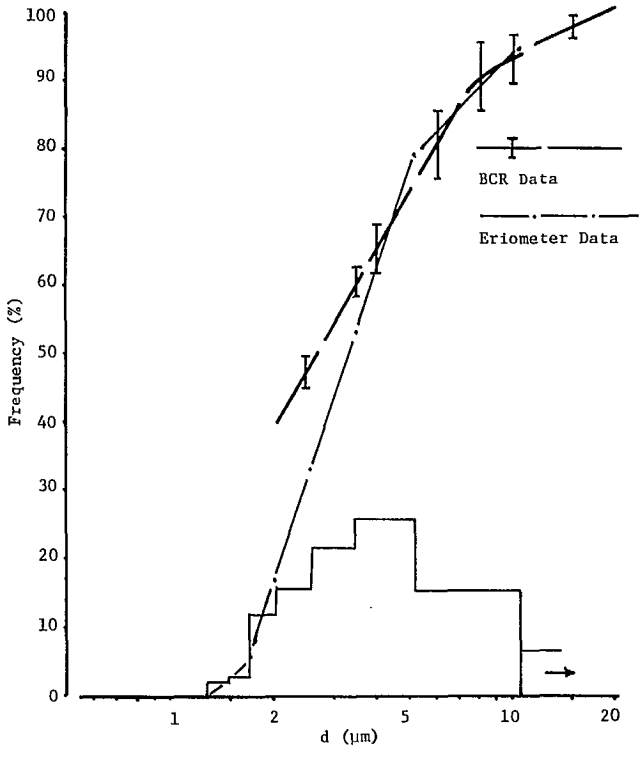

Fig. 16 - Distribution for silica sample, BCR 67

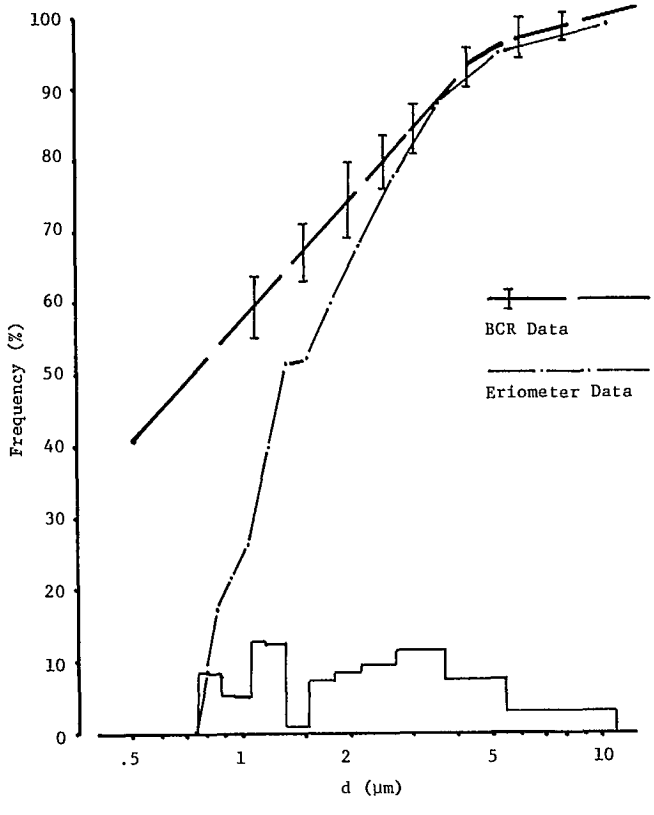

Fig. 18 - Distribution for silica sample, BCR 70

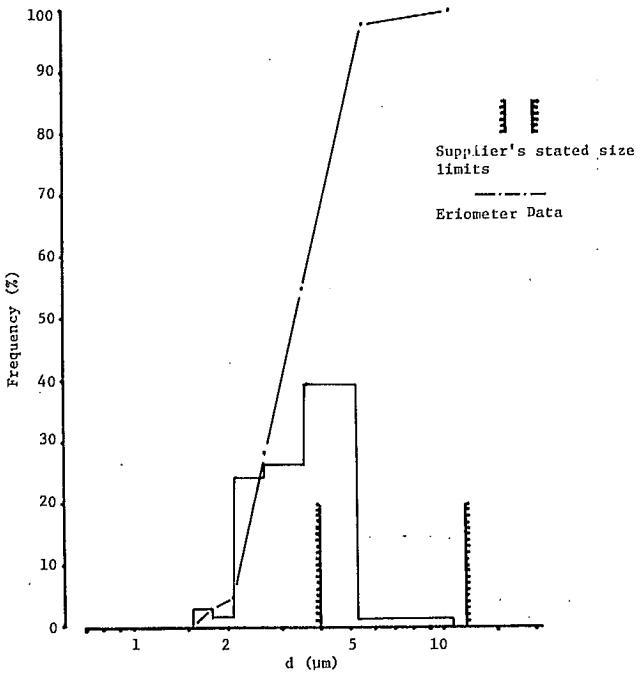

Fig. 19 - Distribution for 4 µm to 12 µm diamond dust

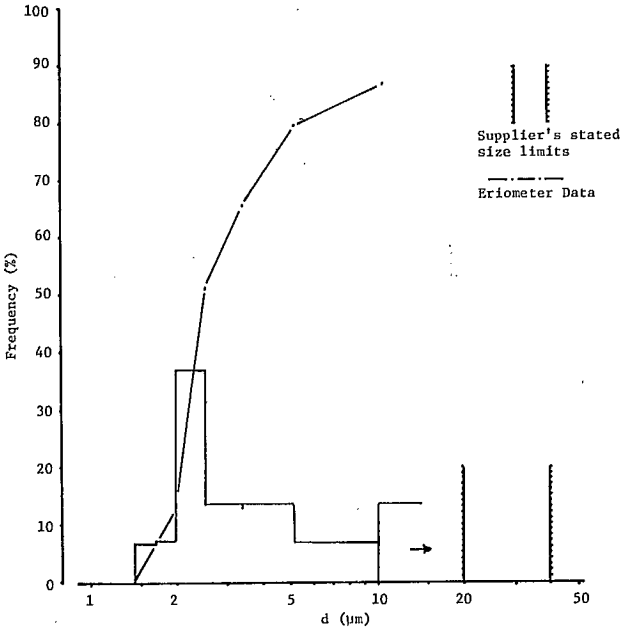

Fig. 21 - Distribution for 20 µm to 40 µm diamond dust (with Z = 37.7 mm)

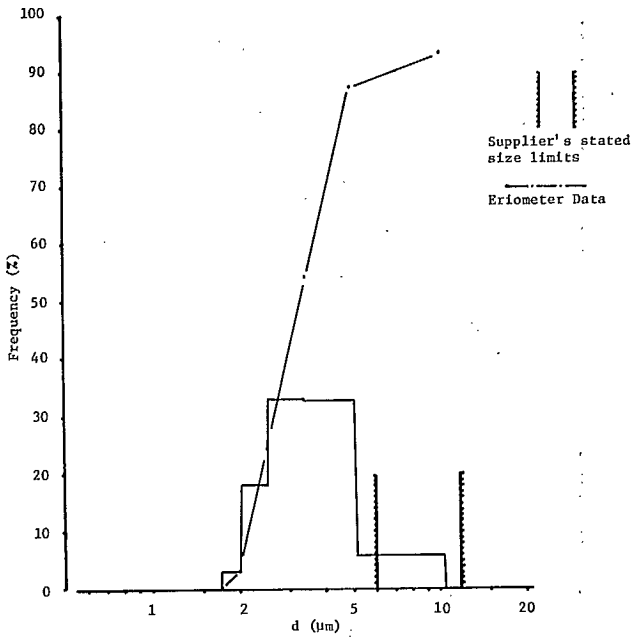

Fig. 20 - Distribution for 6 µm to 12 µm diamond dust

Table 7 - Effects of differential settling of the fineparticles on the diffracted energy

Iris diaphragm radius mm	BCR 67 (3 to 20 µ) L(close)	BCR 67 (3 to 20 µ) L(open)	Diamond dust I (4 to 12 µ) L(close)	Diamond dust I (4 to 12 µ) L(open)
8	100	99.9		
7	99.5	99.4		
6	98.9	98.9	100	99.7
5	98.1	98.0	98.7	98.6
4	96.9	96.8	96.7	96.7
3	92.4	92.3	90.0	89.9
2	84.4	84.4	81.8	81.8
1	67.4	67.4	70.9	70.9
0	0	0	0	0

imentation are based on different phenomena, and for non-spherical fineparticles this will always result in differences in the distribuion curves.

Given the wide range of fineparticle sizes, it is certain there was an overlap of orders in the diffraction pattern. The net result of this would be to overestimate the number of the smallest fineparticles. However, the total energy within the second maximum is less than one-tenth of that in the central maximum and the errors are probably small. In an exact treatment of the error problem, other factors such as number and size of fineparticles must also be considered in determining the relative strengths of the maxima.

There are two serious limitations of this interfacing technique which were encountered in applying it to the silica samples. These were concerned with fineparticles either too small or too large for a proper analysis to be carried out.

The first case is shown in Fig. 15 for silica sample BCR 66, in the size range of 0.35 μm to 2.5 μm. Most of the fineparticles in this sample have diameters between half and twice the wavelength of the incident light. This is below the lower limit to which Fraunhofer diffraction theory applies and, therefore, the analysis of these fineparticles by the use of Eq 5 is not valid. A Mie theory computation could be used to yield information on the fineparticles from their scattering properties (24). This computation would result in a size distribution in terms of equivalent sphere diameters.

A similar problem occurs in silica sample BCR 70 of 0.5 to 12 μm (Fig. 18). The smallest fineparticles were again outside the range of validity for Fraunhofer diffraction theory, and this resulted in an incorrect calculation of the light energy distribution for these fineparticles. However, as the size of fineparticles increased, the effects of this decreased, and the measured and certified distributions were in closer agreement.

The silica sample BCR 69, of 12 to 90 μm, demonstrates the effects of overly large fineparticles (Fig. 17). The central maxima in the diffraction patterns of these fineparticles all fell within the three innermost rings of the interface diaphragm i.e., the scattering is predominantly into small angles. Because of the large size of fineparticles there is a significant amount of energy diffracted into the higher order maxima. Thus, the measurements made at larger aperture radii were from these higher orders and this resulted in a large underestimation of fineparticle size. This problem could be alleviated by expanding the path length, Z in Eq 5, and recalibrating the eriometer.

The three diamond dusts demonstrate another problem which may arise in the eriometric analysis of extremely irregular fineparticles. As seen in Fig. 12 through 14, these diamond fragments contain many sharp corners. The Fourier Transform of such sharp corners consists of high frequency components which correspond to large angle scattering in the Fraunhofer diffraction pattern. The energy thus scattered is interpreted by the analytical procedure as resulting from small spherical fineparticles. As a result, the measured size ranges for the three diamond dusts, as seen in Fig. 19, 20 and 21, are all below those determined microscopically. The problem is further complicated for the 20 to 40 μm sample by the effect of higher order diffraction discussed in connection with silica sample BCR 69.

To verify that an expansion of the scale of the instrument would increase the upper fineparticle size limit, the path length was increased and recalibrated as Z = 200 mm. At this distance the first minimum in the diffraction pattern of the 9.69 μm latex spheres occurs at ρ = 16 mm. The silica sample BCR 69 and the largest diamond dust sample were reanalyzed. The results are given in Table 8 and the distribution curves are given in Fig. 22 and 23. For purposes of comparison, the cumulative curve from the published data is repeated in Fig. 22.

The eriometric analysis of BCR 69 at this expanded scale yields results in reasonable agreement with the certification data. However, the 20 to 40 μm diamond dust sample still ex-

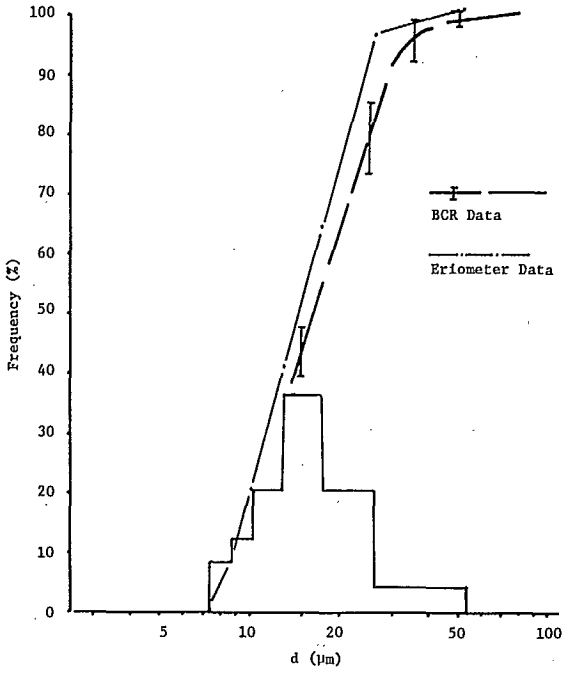

Fig. 22 - Distribution for silica sample BCR 69 (with Z = 200 mm)

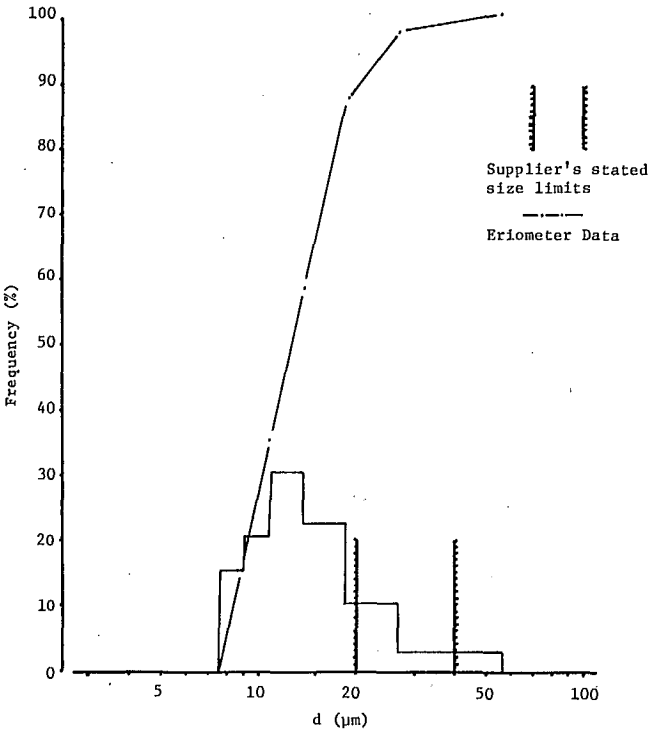

Fig. 23 - Distribution for 20 μm to 40 μm diamond dust (with Z = 200 mm)

hibits the problems arising from the sharp corners. These results, basically are in accord with the earlier discussions.

CONCLUSIONS AND SUGGESTIONS FOR FURTHER RESEARCH EFFORT

An iris diaphragm with focusing lenses has been shown to be a relatively low cost, reliable means of interfacing an eriometer to a data acquisition/processing system. When the eriometric analysis was applied to fineparticles of silica whose size range was adequately covered by the system, the results were in good agreement with those from microscopic analysis.

The difficulties which arise when the fineparticles are predominantly larger than the calibration size range have been demonstrated. Effectively, this results in second or higher orders of diffraction contributing to a gross underestimation of fineparticle size. It has also been shown that errors occur if there are large numbers of fineparticles present with sizes smaller than those to which the analytical theory applies.

The analysis of diamond fragments has shown the effects of extreme irregularities in shape. This results in an underestimation of fineparticle size due to the high frequency scattering components.

The uses of this interface have been demonstrated in sizing monodisperse and polydisperse systems of fineparticles.

It is suggested that further worthwhile development work could be directed to varying the path length and the aperture radius under microprocessor control. This should greatly enhance the ease of operation and the reliability of the interface system. To extend the lower limit of particle sizes which may be analyzed, a more exact analytical process, based on the Mie theory of scattering, could be developed. It should be remembered, however, that these sub-micrometre particles are usually only found as airborne

Table 8 - Analysis of samples with expanded eriometer scale

Ring range mm		Size range µm		BCR 69 12 to 90 µm			Diamond dust 20 to 40 µm		
Max	Min	Min	Max	ΔL	N%	ΣN%	ΔL	N%	ΣN%
8	7	6.83	7.83	0	0	0	0	0	0
7	6	7.83	9.10	0.5	8	8	1	15	15
6	5	9.10	10.9	1.0	12	20	4	20	35
5	4	10.9	13.7	2.5	20	40	11	30	65
4	3	13.7	18.2	12.5	36	76	13.5	22	87
3	2	18.2	27.3	27.0	20	96	25.5	10	97
2	0*	27.3	54.5	56.5	4	10	45.0	3	100

* Because of design constraints, it was not possible to measure the energy at ρ = 1 mm at this expanded scale. The size of 54.5 µm is that which corresponds to ρ = 1 mm and was used in the calculations.

dust, particularly wherever a combustion process is taking place, e.g., diesel exhaust particulates. In the more typical industrial applications, the particle sizes are well above this range.

ACKNOWLEDGEMENTS

The author is indebted to Professor Brian H. Kaye, Department of Physics, Laurentian University, who suggested and supervised this work and to J. Leblanc for assistance with the experimental program. During the course of the study several discussions with Professors N.I. Robb and A.J. Patitsas proved very enlightening. The aid of J. Talbot and A. Webster in the preparation of the original thesis is gratefully acknowledged.

The silica samples studied were supplied by R. Wilson of the Division of Chemical Standards, National Physical Laboratory, Teddington, U.K. The diamond dusts were supplied by the DeBeers Company.

The program was made possible through the cooperation of the Mining Research Laboratories, Canada Centre for Mineral and Energy Technology (CANMET, EMR), in granting part-time leave of absence for studies and the preparation of this report in partial fulfillment of the requirements for a Master of Science degree in Physics.

REFERENCES

1. Kaye, B.H. "Eriometry; lecture notes on rapid response methods for characterizing fineparticle systems"; Wiesbaden; (proceedings to be published); Jan. 1980.

2. Talbot, J.H. "Automated dust measurement: the diffraction size frequency analyzer"; J. Mine Vent Soc S Afr; 20:2; Feb. 1967.

3. Anon. "A laser that sizes up particles"; Bus Week; July 11, 1977.

4. Hickling, R. "Holography of liquid droplets"; Gen Motors Res Pub GMR-869.

5. Wyler, J.S. and Desai, K.J. "Laser light scattering probe"; Ind Res Dev; June 1978.

6. Lieberman, A. "Optical instruments monitor liquid-borne solids"; Chem Eng; Dec. 18, 1978.

7. Brumberger, H., Stein, R.S. and Rowell, R. "Light scattering"; Sci and Technology; Nov. 1968.

8. Weiss, E., and Wertheimer, A. "Theoretical basis for particulate mass measurement by low angle forward light scattering"; Leeds and Northrup; ATN No. 6410-7402; April 1974.

9. Wertheimer A. "Real time measurements of particulate distribution data using low angle forward light scattering"; Leeds and Northrup; ATN No. 6410-7404; Dec. 1974.

10. Cornillaut, J. "Particle size analyzer"; App Optics, 11:2; Feb. 1972.

11. Cochrane, T.S., Knight, G., Richards, L.C. and Stefanich, W. "Comparison of dust sampling instruments"; Research Report R-250; CANMET, Energy, Mines and Resources Canada; Oct. 1971.

12. Talbot, J.H. "A diffraction size frequency analyzer with automatic recording of size frequency distributions and total and respirable surface areas"; Sci Instrum, 43: 1966.

13. Fowles, G.R. "Introduction to modern optics"; Holt, Rinehart and Winston; 1968.

14. Born, M. and Wolf, E. "Principles of optics"; 4th edition; Pergamon Press; 1970.

15. Talbot, J.H. "Fraunhofer diffraction pattern of a random distribution of identical apertures in a plane screen"; Proc Physics Soc; 89; 1966.

16. Thompson, B.J. "Diffraction by opaque and transparent particles"; Soc Photo Instrum Eng; Aug. 1963.

17. Silverman, B.A., Thompson, B.J. and Ward, J.H. "A laser fog disdrometer"; Appl Meteor; 3; 6; Dec. 1964.

18. Felton, P.G. "Instream measurement of particle size distribution"; Proc Internat Symp Instream Meas Partic Solid Prop; Christen Michelson Institute, Bergen, Norway; Aug. 1978.

19. Felton, P.G. "Measurement of particle/droplet size distributions by a laser diffraction technique"; Particle Size Analysis Conference, Nuremberg, West Germany; (proceedings to be published); Sept. 1979.

20. Hodkinson, J.R. "Particle sizing by means of the forward scattering Lobe"; Proc Optic Soc Amer; 1965.

21. McSweeney, A. "An optical transform technique for measuring the size distribution of particles in fluids"; National Bureau of Standards; 1974.

22. Wilson, R. "Some recently certified particle size reference materials"; Particle Size Analysis Conference, Nuremberg, West Germany; (proceedings to be published); Sept. 1979.

23. Robb, N.I., Laurentian University; private communication.

24. Patitsas, A.J. "A simple method for determining the size of a sphere from the extrema of the scattering intensity"; Colloid and Interface Sci, 45:2; 1973.

APPENDIX A - COMPUTER ANALYSIS OF DATA

The following pages outline the approach used in the computer analysis of the data. Where necessary, additional explanatory notes are given. Throughout this discussion, the subscript i is used to denote fineparticle size effects and j denotes aperture size effects.

STEP 1: Input experimental values of ρj, ΔLj and Z

STEP 2: Compute the values of fineparticle diameter, D_i, from:

$$D_i = \frac{1.357\lambda Z}{\Pi \rho_j}$$

Note: Following the treatment by Felton (A1) and Robb (A2), the energy falling within an annulus may be expressed as:

$$E = \int_0^{2\Pi} \int_{\rho}^{\rho+\Delta\rho} I\, \rho d\rho d\phi$$

Provided $\Delta\rho$ is very small, the intensity across the annulus may be regarded as constant and the integral evaluated as:

$$E = I\,(2\Pi\rho)\,\Delta\rho$$

$$\text{or } E = I_o\left[\frac{2J_1(S)}{S}\right]^2 (2\Pi\rho)\,\Delta\rho$$

As $S = \Pi D\rho/\lambda Z$; this expression may be written:

$$E = K\,\frac{J_1^{\,2}(S)}{S}\,\Delta S$$

with K = constant

The maximum energy occurs at:

$$\frac{dE}{dS} = 0$$

Evaluation of this derivative may be carried out as follows:

$$\frac{dE}{dS} = \frac{d}{dS}\left[\frac{KJ_1^{\,2}(S)}{S}\,\Delta S\right]$$

$$\frac{dE}{dS} = K\left[\frac{S[2J_1(S)]\frac{d\,[J_1(S)]}{dS} - J_1^{\,2}(S)}{S^2}\right]\Delta S + \frac{KJ_1^{\,2}(S)}{S}\,\frac{d(\Delta S)}{dS}$$

As ΔS may be regarded as a constant, the second term vanishes. Furthermore:

$$\frac{d}{dS}\,[J_1(S)] = J_o(S) = \frac{1}{S}\,J_1(S)$$

$$\frac{dE}{dS} = K\Delta S\left[\frac{2S\,J_1(S)\,[J_o(S) - (1/S)\,J_1(S)] - J_1^{\,2}(S)}{S^2}\right]$$

$$\frac{dE}{dS} = K\Delta S\,\frac{J_1(S)}{S^2}\,[2S\,J_o(S) - 3J_1(S)] = 0$$

There are three possible solutions to this equation:

$$\Delta S = 0$$

$$\frac{J_1(S)}{S^2} = 0$$

$$\frac{J_1(S)}{J_o(S)} = \frac{2S}{3}$$

The first two of these are not physically meaningful solutions. The annulus has a non-zero width, although small. The point at which $J_1(S) = 0$ corresponds to a minimum in the diffracted intensity and cannot, therefore, correspond to the maximum contribution to the energy within the annulus.

The third solution is satisfied at S = 1.357. This results in the calculation of fineparticle sizes on the basis of maximum contributions to energy in a

given annulus. In the paper by Felton the result is given as S = 1.375 (A1). This difference is believed due to a transcription error.

STEP 3: Compute the theoretical inversion matrix T_{ij} as follows:

(i) starting with the smallest value, hold D_i constant

(ii) determine the contribution to the energy of the j'th ring from this size of fineparticle using:

$$T_{ij} = J_o^2 (S_{i,j-1}) + J_1^2 (S_{i,j-1}) - J_o^2 (S_{ij}) - J_1^2 (S_{ij})$$

$$S_{ij} = \frac{\pi D_i \rho_j}{\lambda Z}$$

Note: The Bessel functions $J_o(x)$ and $J_1(x)$ may be evaluated from the Chebyshev polynomial approximations (A3):

$$J_o(x) = 1 - 2.250(x/3)^2 + 1.266(x/3)^4 - 0.3164(x/3)^6 + \ldots$$

$$J_1(x) = x\,[1/2 - 0.5625(x/3)^2 + 0.2109(x/3)^4 - 0.395(x/3)^6 + \ldots]$$

valid for $|x| \leq 3$

(iii) reset D_i to the next largest value and repeat the above procedure.

STEP 4: Assume that the outermost ring contains energy diffracted only by the smallest fineparticles. The contributions of these fineparticles to all rings can be determined by normalizing the values calculated in Step 3 to the observed energy in the outermost ring:

$$E_{ij} = \frac{T_{ij}\,\Delta L_i}{T_{ii}} \qquad \text{(i constant)}$$

As i is fixed for the given fineparticle size the normalization factor $(\Delta L_i / T_{ii})$ is a constant for each size. Note that so far only one column of the T_{ij} matrix is normalized to the observed values.

STEP 5: The total energy diffracted by the smallest fineparticles is determined by summing the values from Step 4:

$$E_i = \sum_j E_{ij}$$

STEP 6: The total energy is used to compute the number of fineparticles of this size:

$$N_i = E_i / D_i^2$$

Note: From Eq 4, the total energy, E_i, diffracted by a group of fineparticles is proportional to the number of fineparticles, N_i, and to the square of their diameter, D_i^2. In Steps 4 and 5, the total diffracted energy was determined for a single size of fineparticle - the smallest size. As such, Eq 3 is applicable to the energy distribution from this size of fineparticle. The present task, however, does not require knowledge of the actual energy distribution, but considers only the total diffracted energy - E in Eq 3 - which is given by the calculated value of E_i.

STEP 7: The contributions from the smallest fineparticles are subtracted from the observed values. Remembering that i is fixed for this fineparticle size, these contributions are given by a single column in the inversion matrix E_{ij}. Extracting this column:

$$C_j = E_{ij} \qquad i = \text{constant (from Step 4)}$$

allows the subtraction to be carried out:

$$\Delta L_j \leftarrow \Delta L_j - C_j$$

This results in the outermost ring having no residual energy and the maximum value of ρ_j decreasing by one step.

STEP 8: Return to Step 4 and repeat the procedure for each size of fineparticle.

STEP 9: The number of fineparticles of each size is normalized:

$$\sum_i N_i = 100$$

STEP 10: Output values of D_i and N_i.

REFERENCES

A1: Felton, P.G. "Measurement of particle/droplet size distributions by a laser diffraction technique"; Part Size Anal Conf, Nuremberg, West Germany; (Proceedings to be published), Sept. 1979.

A2: Robb, N.I. Laurentian University; private communication.

A3: U.S. Bureau of Standards "Handbook of mathematical functions"; Abramowitz and Stegun (eds), Washington Government Printing Office; p 369; 1964.

OPINION POLL

The opinion of concerned readers may influence the direction of future CANMET research.

We invite your assessment of this report - No._____

Is it useful?	Yes_____	No_____
Is it pertinent to an industry problem?	Yes_____	No_____
Is the subject of high priority?	Yes_____	No_____

Comments_____

_____

_____

Please mail to: CANMET Editor, EMR, 555 Booth Street,
Ottawa, Ontario, K1A 0G1

A complimentary copy of the CANMET REVIEW describing CANMET research activity will be sent on request.

CANMET REPORTS

Recent CANMET reports presently available or soon to be released through Printing and Publishing, Supply and Services, Canada (addresses on inside front cover), or from CANMET Publications Office, 555 Booth Street, Ottawa, Ontario, K1A 0G1:

Les récents rapports de CANMET, qui sont présentement disponibles ou qui le seront bientôt peuvent être obtenus de la direction de l'Imprimerie et de l'Edition, Approvisionnements et Services Canada (adresses au verso de la page couverture), ou du Bureau de vente et distribution de CANMET, 555, rue Booth, Ottawa, Ontario, K1A 0G1:

80-7E Release of lead from typical pottery glaze formulation; D.H.H. Quon and K.E. Bell;
Cat. No. M38-13/80-7E, ISBN 0-660-10688-4; Price: $1.75 Canada, $2.10 other countries.

80-8 Metals terminology/La terminologie des mètaux; André Blouin;
Cat. No. M38-13/80-8, ISBN 0-660-50586-X; Price: $24.95 Canada, $29.95 other countries.

80-9E SU-1a: A certified nickel-copper-cobalt reference ore; H.F. Steger and W.S. Bowman;
Cat. No. M38-13/80-9E, ISBN 0-660-10714-7; Price: $1.95 Canada, $2.35 other countries.

80-10E DL-1a: A certified uranium-thorium reference ore; H.F. Steger and W.S. Bowman;
Cat. No. M38-13/80-10E, ISBN 0-660-10715-5; Price: $1.50 Canada, $1.80 other countries.

80-11E Mineral insulation - A critical study; A.A. Winer and S.B. Wang;
Cat. No. M38-13/80-11E, ISBN 0-660-10683-3; Price: $2.00 Canada, $2.40 other countries.

80-12E Mineral waste resources of Canada Report No. 4 - Mining wastes in the Atlantic provinces; R.K. Collings;
Cat. No. M38-13/80-12E, ISBN 0-660-10689-2; Price: $1.95 Canada, $2.35 other countries.

80-13E Mineral waste resources of Canada Report No. 6 - Mineral wastes as potential fillers; R.K. Collings;
Cat. No. M38-13/80-13E, ISBN 0-660-10699-X; Price: $2.25 Canada, $2.70 other countries.

80-14E The corrosion of welds in ice-breaking ships - A review; J.B. Gilmour;
Cat. No. M38-13/80-14E, ISBN 0-660-10700-7; Price: $1.25 Canada, $1.50 other countries.

80-15 Catalogue of CANMET publications 1979/80/Catalogue des publications de CANMET 1979/80; compiled by J.L. Metz, French translation by J. Collins-DeCotret;
Cat. No. M38-13/80-15, ISBN 0-660-50725-0; Price: $6.00 Canada, $7.20 other countries.

80-16E Synthesis and characterization of potassium ion conductors in the system K_2O-Al_2O_3-TiO_2; D.H.H. Quon and T.A. Wheat;
Cat. No. M38-13/80-16E, ISBN 0-660-10747-3; Price: $2.50 Canada, $3.00 other countries.

80-17E CANMET review 1979/80; TID staff;
Cat. No. M38-13/80-17E, ISBN 0-660-10835-6; Price: $5.00 Canada, $6.00 other countries.

80-18E Durability of concrete containing granulated blast furnace slag or fly ash or both in marine environment; V.M. Malhotra, C.G. Carette and T.W. Bremner;
Cat. No. M38-13/80-18E, ISBN 0-660-10701-5; Price: $2.00 Canada, $2.40 other countries.

80-19E Mineral waste resources of Canada Report No. 7 - Ferrous metallurgical wastes; R.K. Collings and S.S.B. Wang;
Cat. No. M38-13/80-19E, ISBN 0-660-10748-1; Price: $2.50 Canada, $3.00 other countries.

80-21E English-French glossary of mining and related terms/Glossaire Français-Anglais des termes miniers et du vocabulaire connexe; A.S. Romaniuk, updated and translated by I. Slowikowski;
Cat. No. M38-13/80-21, ISBN 0-660-50723-4; Price: $5.00 Canada, $6.00 other countries.

80-23E Thermal hydrocracking of Athabasca bitumen: Comparison of computer simulated values of feed and products vaporization with CANMET pilot plant data; D.J Patmore and B.B. Pruden;
Cat. No. M38-13/80-23E, ISBN 0-660-10237-4; Price: $2.25 Canada, $2.70 other countries.